

Synthesis and Nonlinear Optical Properties of Side Chain Liquid Crystalline Polymers Containing Azobenzene Push–Pull Chromophores

RAQUEL ALICANTE,¹ RAFAEL CASES,¹ PATRICIA FORCÉN,² LUIS ORIOI,² BELÉN VILLACAMPA¹

¹Dept. Física de la Materia Condensada, Facultad de Ciencias-Instituto de Ciencia de Materiales de Aragón, Universidad de Zaragoza-CSIC, Pedro Cerbuna 12, Zaragoza 50009, Spain

²Dept. Química Orgánica, Facultad de Ciencias-Instituto de Ciencia de Materiales de Aragón, Universidad de Zaragoza-CSIC, Pedro Cerbuna 12, Zaragoza 50009, Spain

Received 14 September 2009; accepted 5 October 2009

DOI: 10.1002/pola.23776

Published online in Wiley InterScience (www.interscience.wiley.com).

ABSTRACT: Azobenzene monomeric precursors bearing piperazine as donor moiety with different withdrawing groups and derived side chain polymethacrylates have been prepared and characterized. Monomers having terminal cyano or nitro groups, and the corresponding polymers, exhibited smectic A phases. Linear and nonlinear optical properties of every monomer and thin films of the cyano polymer (**pol-PZ-CN**) have been also studied. UV-vis spectroscopy revealed out-of-plane orientation in the as prepared films, as confirmed by waveguide refractive index measurements. Moreover, absorption spectra indicated the presence of azo aggregates in these films. The initial molecular arrangement has been modified by applying thermal annealing within the mesophase range and UV-blue irradiation. Although thermal annealing resulted in a significant

amplification of the out-of-plane optical anisotropy due to thermotropic self-organization of side chain azo moieties, irradiation with 440 nm light induced some disruption of aggregates. The nonlinear optical response of Corona poled films has been studied by second harmonic generation measurements, and the influence of the molecular arrangement on the nonlinear d_{ij} coefficients has been analyzed. The more efficient poling corresponded to preirradiated films. In any case, a noticeable degree of polar order (70% of the initial d_{33} value) remained for several months after the poling in films kept at RT. © 2009 Wiley Periodicals, Inc. *J Polym Sci Part A: Polym Chem* 48: 232–242, 2010

KEYWORDS: azo polymers; d_{ij} coefficients; EFISH; liquid-crystalline polymers (LCP); NLO

INTRODUCTION The study of organic materials with nonlinear optical (NLO) properties involves a great interest for different electrooptical and photorefractive applications. In particular, polymers provide systems with high flexibility due to its synthetic versatility and easy processability.¹ Nevertheless, one of the most studied strategies for designing second order nonlinear polymers not only implies the incorporation of dipolar, highly polarizable donor- π -acceptor molecules (normally used as NLO-phores) into a macromolecular structure but also a noncentrosymmetric organization. The experimental technique generally used for this purpose is based on the electric field poling. In a typical poling process, thin polymer films are heated near glass transition temperature (T_g) under a strong electric field and then cooled to room temperature (RT) with the field on. After the poling process, NLO chromophores show a preferential orientation along the field direction, defining an optical axis perpendicular to the film surface ($C_{\infty v}$ symmetry).

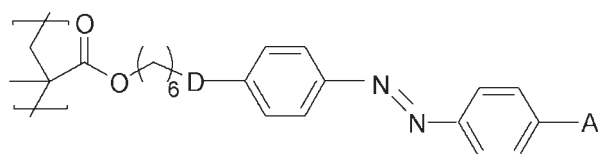
Azobenzene-containing polymers are a really interesting alternative in nonlinear optics.² On the one hand, azobenzene derivatives having appropriate donor and acceptor groups

are stable NLO-phores that can be easily incorporated in polymeric systems both as guest molecules and as a structural part of the side or main chain of polymers. On the other hand, the photoaddressability of these systems can play an important role in assisting chromophore alignment.³ On illumination with light of appropriate wavelength, azobenzene moieties undergo E-Z reversible isomerization and the molecular motion of NLO-phores is enhanced, so it is possible to align them along an applied DC electric field at temperatures well below the T_g of the polymer. This process that combines light and electrical poling is known as photo-assisted poling (PAP),⁴ and it allows inducing NLO properties on azopolymers while avoiding thermal decomposition.

We have previously reported the photo-induced anisotropy⁵ and nonlinear optical properties of side chain liquid crystalline polymers (SCLCP) having 4-alkoxy-4'-cyanoazobenzene derivatives as chromophores. Concerning nonlinear properties, a stable polar order and, consequently, NLO response was achieved in a series of methacrylic homo and copolymers with different azo content.^{5(b)} Higher response is

Correspondence to: B. Villacampa (E-mail: bvillaca@unizar.es)

Journal of Polymer Science: Part A: Polymer Chemistry, Vol. 48, 232–242 (2010) © 2009 Wiley Periodicals, Inc.



Nomenclature	Donor (D)	Acceptor (A)
pol-O-CN	-O-	-CN
pol-PZ-CN		-CN
pol-PZ-NO ₂		-NO ₂
pol-PZ-DCN		

SCHEME 1 Polymers synthesized for the study.

expected to be obtained if more efficient chromophores are incorporated into the polymer, provided that a efficient polar orientation of NLO moieties is induced by the electric field. It has been well established that dipolar interactions between guests NLO chromophores dispersed in a polymeric matrix attenuate noncentrosymmetric order.⁶ Aggregation, as a consequence of these interactions, is a detrimental factor for electric poling efficiency and isotropic poled polymer model⁷ does not explain the observed NLO macroscopic response, even at moderate chromophore loading. The role of dipole moment and chromophore concentration in hindering polar order has been also discussed in side chain azopolymers.⁸ On the other hand, the liquid crystalline character has been predicted to enhance field-induced polar order.⁹ Experimental results supporting this statement were published by several authors.¹⁰ However, it has been also reported the failure in poling smectic A SCLCP¹¹ because of the strong dipole-dipole interactions.

In this work, we present the synthesis, characterization, and study of the NLO properties of a series of liquid crystalline monomers and polymers having azobenzene chromophores with a strong donor group as piperazine (linked by N to azo unit) and different acceptor groups (Scheme 1). Side-chain polymethacrylates with similar chromophores directly linked to the main chain had been studied by Tirelli et al.¹² obtaining a weak macroscopic NLO response, fairly lower than the observed one for the same chromophores dispersed into a polymeric matrix. As it is expected that the use of flexible spacers in the side chain would improve the orientability and consequently the nonlinear response, the piperazine donor group existing in our monomeric precursors is separated from the methacryloyl moiety by a hexamethylene spacer. The configuration of the polymeric system makes a high NLO response predictable and allows getting a deeper insight into the influence that liquid crystalline properties have on nonlinear optical response. Thermal and mesomorphic properties of monomers and derived polymers will be described.

Monomer hyperpolarizabilities have been determined in solution. Thin films of **pol-PZ-CN** have been prepared and poled by Corona discharge, to induce second order NLO properties. For a better understanding of the competition in alignment between intermolecular and external forces, we have included some results concerning a previously reported monomer and the corresponding polymer¹³ (**mon-O-CN** and **pol-O-CN**, respectively, see Scheme 1), which have been measured under equivalent experimental conditions. Diverse treatments have been applied to polymer films of different thickness, in particular thermal annealing at temperatures within the mesophase range and/or UV-blue light irradiation. Special attention has been paid to the role that this previous processing, which modifies the molecular arrangement and aggregation state of the films, plays on their final NLO response, characterized by second order d_{ij} coefficients.

EXPERIMENTAL

Synthesis

6-Chlorohexanol, 4-nitroaniline, 4-cyanoaniline, and methacryloyl chloride were purchased from Aldrich and used without previous purification. 4-Aminobenzaldehyde was prepared from *N*-(4-formylphenyl) acetamide according to a previously reported method.¹⁴

Synthesis of Monomers

N-(6-Hydroxyhexyl)-*N'*-Phenylpiperazine (**1**)

Phenylpiperazine (31 mmol), 32 mmol of 6-chloro-1-hexanol, 31 mmol of K₂CO₃, and 1 mmol of KI were mixed in 50 mL of acetone. The reaction mixture was refluxed overnight, cooled to room temperature, and finally filtered to remove inorganic salts. The solvent was removed by evaporation under vacuum to obtain the crude, which was purified by column chromatography on silica gel using dichloromethane/methanol (9:1) as eluent and then washed with hexane.

Yield: 50%. ELEM. ANAL. (calculated): %C 74.19 (73.42), %H 9.43 (9.99), %N 10.38 (10.68). IR (NaCl, Nujol, cm⁻¹): 3290–3219 (OH); 1598, 1500 (Ar); 1244 (C–O). ¹H-NMR (CDCl₃) δ /ppm: 7.28–7.24 (m, 2H), 6.9 (d, J = 8.8 Hz, 2H), 6.8 (t, J = 7 Hz, 1H), 3.6 (t, J = 1.6 Hz, 2H), 3.2 (m, 4H), 2.6 (m, 4H), 2.41 (t, J = 8 Hz, 2H), 1.62–1.55 (m, 4H), 1.43–1.37 (m, 4H).

N-(6-Hydroxyhexyl)-*N'*-[(4-*X*-Phenyl)Azophenyl] Piperazine, *X* = CN (**2**), NO₂ (**3**), COH (**4**)

Obtained through diazonium coupling between *N*-(hydroxyhexyl)-*N'*-phenylpiperazine (**1**) and the diazonium salt of 4-cyanoaniline, 4-nitroaniline or 4-aminobenzaldehyde: 4 mmol of the corresponding aniline was dissolved in a mixture of water (100 mL) and HCl (45 mL) and cooled in an ice bath under stirring. A solution of NaNO₂ (4 mmol) in water (10 mL) was added drop wise keeping the temperature under 5 °C, and finally *N*-(hydroxyhexyl)-*N'*-phenylpiperazine was added to the mixture. The reaction was running at room temperature for 24 h. The resulting solution was added to a Na₂CO₃ saturated dissolution, and the precipitated was filtered and rinsed with water. The crude product was finally purified by column chromatography on silica gel using methylene chloride/methanol (9:1) as eluent.

(2): Yield: 40%. ELEM. ANAL. (calculated): %C 70.38 (70.56), %H 7.36 (7.47), %N 17.63 (17.89). IR (NaCl, Nujol, cm^{-1}): 3542 (OH); 2225 (CN); 1600, 1515, (Ar); 1235, 1141 (C—O); 850 (Ar). $^1\text{H-NMR}$ (CDCl_3) δ /ppm: 7.84–7.83 (m, 4H), 7.7 (d, $J = 8.4$ Hz, 2H), 6.9 (d, $J = 9.2$ Hz, 2H), 3.6 (t, $J = 6.8$ Hz, 2H), 3.73–3.33 (m, 4H), 2.55–2.52 (m, 4H), 2.34 (t, $J = 7.4$ Hz, 2H), 1.52–1.49 (m, 4H), 1.33–1.32 (m, 4H). **(3):** Yield: 54%. ELEM. ANAL. (calculated): %C 64.18 (64.21), %H 7.12 (7.10), %N 16.95 (17.02). IR (NaCl, Nujol, cm^{-1}): 3224 (OH); 1602, 1507, (Ar); 1235, 1141 (C—O); 857 (Ar). $^1\text{H-NMR}$ (CDCl_3) δ /ppm: 8.3 (d, $J = 9$ Hz, 2H), 7.95–7 (m, 4H), 6.95 (d, $J = 9$ Hz, 2H), 3.65 (t, $J = 6.4$ Hz, 2H), 3.44–3.41 (m, 4H), 2.61–2.58 (m, 4H), 2.4 (t, $J = 7.6$ Hz, 2H), 1.58–1.55 (m, 4H), 1.4–1.38 (m, 4H). **(4):** Yield: 40%. ELEM. ANAL. (calculated): %C 70.18 (70.02), %H 7.52 (7.66), %N 14.55 (14.20). IR (KBr pellet, cm^{-1}): 3423 (OH); 2779 (HC=O); 1688 (HC=O); 1593, 1506, 1380 (Ar); 1233, 1141 (C—O); 839 (Ar). $^1\text{H-NMR}$ (CDCl_3) δ /ppm: 10.07 (s, 1H), 8–7.98 (m, 4H), 7.92–7.9 (d, $J = 8$ Hz, 2H), 6.98–6.96 (d, $J = 8$ Hz, 2H), 3.68–3.64 (t, $J = 6.8$ Hz, 2H), 3.49 (s, 1H), 3.44–3.41 (m, 4H), 2.62–2.59 (m, 4H), 2.43–2.4 (t, $J = 7.2$ Hz, 2H), 1.59–1.54 (m, 4H), 1.4–1.39 (m, 4H).

***N*-(6-Methacryloyloxyhexyl)-*N'*-[4-(4'-*X*-Phenyldiazenyl)-phenyl] Piperazine, *X* = CN (mon-PZ-CN), NO_2 (Mon-PZ- NO_2), COH (5)**

The monomers **mon-PZ-CN**, **mon-PZ- NO_2** and the precursor **(5)** were obtained by condensation of the corresponding compound **(2)**, **(3)**, or **(4)** and methacryloyl chloride in freshly distilled THF: 1.5 mmol of hydroxy derivative **(3)**, **(4)**, or **(5)** and 2.2 mmol of methacryloyl chloride were dissolved in 250 mL of distilled THF, to which triethylamine (2.19 mmol) and 2 mg of inhibitor (2, 6-di-*tert*-butyl-*p*-cresol) were added. The reaction mixture was refluxed under argon for 24 h and then cooled. Water (200 mL) was added, and the solution was extracted with ethyl acetate, the organic layer was dried with anhydrous MgSO_4 . The solvent was removed by evaporation in vacuum. The resulting product was purified from column chromatography on silica gel using methylene chloride/methanol (9:1) as eluent. The monomers were finally recrystallized from ethanol and dried under vacuum.

Mon-PZ-CN. Yield: 60%. ELEM. ANAL. (calculated): %C 70.68 (70.56), %H 7.30 (7.24), %N 15.02 (15.24). IR (KBr pellet, cm^{-1}): 1719 (C=O); 1635 (C=C); 1561, 1506 (Ar); 1235, 1140 (C—O); 848 (Ar). $^1\text{H-NMR}$ (CDCl_3) δ /ppm: 7.84–7.83 (m, 4H), 7.69 (d, $J = 7.6$ Hz, 2H), 6.89 (d, $J = 8.4$ Hz, 2H), 6.03 (s, 1H), 5.48 (s, 1H), 4.08 (t, $J = 6.8$ Hz, 2H), 3.37–3.34 (m, 4H), 2.54–2.51 (m, 4H), 2.33 (t, $J = 7.2$ Hz, 2H), 1.88 (s, 3H), 1.63–1.61 (m, 2H), 1.5–1.47 (m, 2H), 1.35–1.33 (m, 4H).

Mon-PZ- NO_2 . Yield: 80%. ELEM. ANAL. (calculated): %C 64.95 (65.12), %H 6.75 (6.94), %N 14.18 (14.60). IR (KBr pellet, cm^{-1}): 1718 (C=O); 1635 (C=C); 1598, 1515 (Ar); 1235, 1141 (C—O); 857 (Ar). $^1\text{H-NMR}$ (CDCl_3) δ /ppm: 8.27–8.25 (d, $J = 9.2$ Hz, 4H), 7.88–7.83 (m, 4H), 6.9 (d, $J = 9.2$ Hz, 2H), 6.03 (s, 1H), 5.48 (s, 1H), 4.08 (t, $J = 6.8$ Hz, 2H), 3.38–3.35 (m, 4H), 2.54–2.51 (m, 4H), 2.33 (t, $J = 7.2$ Hz, 2H),

1.88 (s, 3H), 1.61–1.59 (m, 2H), 1.5–1.47 (m, 2H), 1.35–1.33 (m, 4H).

(5): Yield: 52%. ELEM. ANAL. (calculated): %C 70.91 (70.10), %H 7.30 (7.41), %N 12.60 (12.11). IR (KBr pellet, cm^{-1}): 2816, 2778 (HC=O); 1711 (C=O); 1694 (HC=O); 1632 (C=C); 1596, 1505 (Ar); 1232, 1133 (C—O); 841 (Ar). $^1\text{H-NMR}$ (CDCl_3) δ /ppm: 10 (s, 1H), 7.94–7.9 (m, 4H), 7.84 (d, $J = 8.8$ Hz, 2H), 6.9 (d, $J = 9.2$ Hz, 2H), 6.03 (s, 1H), 5.48 (s, 1H), 4.08 (t, $J = 6.8$ Hz, 2H), 3.37–3.34 (m, 4H), 2.54–2.51 (m, 4H), 2.33 (t, $J = 7.2$ Hz, 2H), 1.88 (s, 3H), 1.65–1.63 (m, 2H), 1.5–1.47 (m, 2H), 1.35–1.33 (m, 4H).

***N*-(6-Methacryloyloxyhexyl)-*N'*-[4-(4'-(2,2-Dicyanovinyl)-Phenyldiazenyl)phenyl] Piperazine Mon-PZ-DCN**

The monomer **mon-PZ-DCN** was prepared by mixing 1.73 mmol of **(5)**, 2.09 mmol of malononitrile, a few drops of NaOH 1% in 40 mL of ethanol, and 2 mg of inhibitor (2,6-di-*tert*-butyl-*p*-cresol). The mixture was refluxed overnight. The solvent was then evaporated in vacuum, and the monomer was purified by column chromatography using methylene chloride/methanol (9:1) as eluent and finally recrystallized from ethanol.

Yield: 73%. ELEM. ANAL. (calculated): %C 70.38 (70.56), %H 6.32 (6.71), %N 16.40 (16.46). IR (KBr pellet, cm^{-1}): 2225 (CN); 1715 (C=O); 1635 (C=C); 1597, 1513 (Ar); 1383, 1243 (C—O), 837 (Ar). $^1\text{H-NMR}$ (CDCl_3) δ /ppm: 8.3 (d, $J = 8.4$ Hz, 2H), 7.96–7.9 (m, 4H), 6.96 (d, $J = 8.8$ Hz, 2H), 6.1 (s, 1H), 5.55 (s, 1H), 4.14 (t, $J = 6.8$ Hz, 2H), 3.44–3.41 (m, 4H), 2.4 (t, $J = 7.2$ Hz, 2H), 1.95 (s, 3H), 1.70–1.68 (m, 2H), 1.57–1.55 (m, 2H), 1.40–1.38 (m, 4H).

Synthesis of Polymers

Polymers were synthesized by free radical polymerization. The corresponding monomer and AIBN (2.5% w/w in the case of **pol-PZ-CN**, 3% w/w in the case of **pol-PZ- NO_2** and 5% w/w in the case of **pol-PZ-DCN**, see text), as a thermal initiator, were dissolved in 10 mL of freshly distilled DMF. Oxygen was removed by three freeze-pump-thaw cycles by applying vacuum and backfilling with argon. The mixture was immersed into a silicon oil bath, preheated to 70 °C. The reaction was maintained from 48 to 72 h, and the reaction was then cooled to room temperature and poured into ethanol. The solid was isolated by filtration. The polymers were thoroughly washed by using a Soxhlet extractor.

Pol-PZ-CN

Yield: 40%. ELEM. ANAL. (calculated): %C 70.71 (70.56), %H 7.32 (7.24), %N 15.13 (15.24). IR (KBr pellet, cm^{-1}): 2222 (CN); 1723 (C=O); 1597, 1507, (Ar); 1233, 1155 (C—O); 846 (Ar). $^1\text{H-NMR}$ (CDCl_3) δ /ppm: 7.86–7.85 (m, 4H), 7.73–7.72 (m, 2H), 6.91–6.90 (m, 2H), 3.97–3.95 (m, 2H), 3.37–3.36 (m, 4H), 2.57–2.55 (m, 4H), 2.38–2.35 (m, 2H), 1.64–0.86 (m, 13H). $M_n = 10,400$, $M_w/M_n = 1.2$.

Pol-PZ- NO_2

Yield: 42%. ELEM. ANAL. (calculated): %C 65.21 (65.12), %H 6.89 (6.94), %N 14.12 (14.60). IR (KBr pellet, cm^{-1}): 1721 (C=O); 1598, 1514, (Ar); 1235, 1140 (C—O); 857 (Ar). $^1\text{H-NMR}$ (CDCl_3) δ /ppm: 8.34–8.31 (m, 2H), 7.93–7.89 (m, 4H),

6.97–6.90 (m, 2H), 3.99–3.95 (m, 2H), 3.42–3.39 (m, 4H), 2.59–2.58 (m, 4H), 2.40–2.38 (m, 2H), 1.67–0.88 (m, 13H). $M_n = 2300$; $M_w/M_n = 1.7$.

Pol-PZ-DCN

Yield: 35%. ELEM. ANAL. (calculated): %C 70.23 (70.56), %H 6.41 (6.71), %N 16.26 (16.46). IR (KBr pellet, cm^{-1}): 2189 (CN); 1725 (C=O); 1672 (C=C); 1597, 1507, (Ar); 1230, 1139 (C–O), 823 (Ar).

Characterization Techniques

Elemental analyses were performed using a Perkin–Elmer 240C microanalyzer. IR spectra were obtained on a Nicolet Avatar 360-FTIR. ^1H -NMR spectra were measured at room temperature with a Bruker AV-400 spectrometer (spectrum of **pol-PZ-DCN** was not registered because of its poor solubility). Molecular weights and polydispersities were measured by GPC using a Waters 600E HPLC (Waters Styragel columns HR2 and HR4) with a UV Waters 991 photodiode array detector. THF was used as the eluent, and standard samples of polystyrene were used. Thermogravimetric analysis (TGA) was performed using a TA Q5000IR instrument at a heating rate of $10\text{ }^\circ\text{C min}^{-1}$ under a nitrogen atmosphere. Mesogenic behavior was evaluated by polarized-light optical microscopy using an Olympus BH-2 polarizing microscope fitted with a Linkam THMS600 hot stage. Thermal transitions were determined by differential scanning calorimetry (DSC) using a TA DSC Q-1000 instrument under a nitrogen atmosphere with samples sealed in aluminum pans. Glass transition temperatures (T_g) were determined at the midpoint of the baseline jump, and the melting or mesophase-isotropic transition temperatures were read at the maximum of the corresponding peaks. Powdered samples of about 3 mg were used.

Film Preparation and Optical Measurements

Thin films for optical measurements were produced by casting a solution of the polymer in dichloromethane onto clean ITO (Indium Tin Oxide) coated glass substrates. Before film casting and as the last step of the cleaning process, substrates were ozone exposed in a UV photo reactor. Among all the polymers synthesized for this study, only **pol-PZ-CN** samples had suitable quality for optical measurements. In the case of **pol-PZ-NO₂**, brittle films with a poor optical quality were obtained probably due to its low molecular weight. On the other hand, the low solubility of **pol-PZ-DCN** precluded film processing. **Pol-PZ-CN** and **pol-O-CN** films were dried at $40\text{ }^\circ\text{C}$ overnight to eliminate the residual solvent and then stored in the dark. Two groups of films with different thickness, about $0.6\text{ }\mu\text{m}$ and $1.2\text{ }\mu\text{m}$ thick, respectively, were prepared. Refractive indices measurements were performed in a Metricon instrument in which a prism coupler was used to obtain guided wave spectra at different wavelengths: 633, 780 nm, and $1.31\text{ }\mu\text{m}$. The use of light of TE and TM polarization allowed us to determine n_E (ordinary index, in-plane), n_M (extraordinary index, normal to the film surface) and film thickness. An independent thickness measurement was performed using a Veeco Dektak³ST contact profilometer.

Optical absorption measurements were performed in a Cary 500 UV-Vis-NIR spectrophotometer. Linear (vertical/horizontal) polarization of the measuring beam was achieved using a Glan-Thompson prism. The films were held in a rotatory mount (around a vertical axis, perpendicular to the incidence plane), and the absorption spectra were registered at normal and oblique incidence (0° and 45° , respectively).

Nonlinear Optical Measurements

Nonlinear optical characterization was carried out in a NLO Spectrometer from Sopra. Molecular hyperpolarizabilities ($\mu\beta$ values) were measured in solution by using the electric field induced second harmonic (EFISH) generation technique at 1.06 and $1.91\text{ }\mu\text{m}$. The latter was obtained from a H_2 Raman shifter pumped by a Q-switched Nd:YAG laser emitting at $1.06\text{ }\mu\text{m}$. The laser repetition rate was 10 Hz and the pulse width 8 ns. The fundamental light was split in two beams. The less intense one was directed to a *N*-(4-nitrophenyl)-(L)-prolinol (NPP) powder sample whose SH signal was used as a reference to correct laser fluctuations. The other beam was focused onto a wedge shaped EFISH cell, containing the liquid sample (NLO-phore solution). The voltage applied across the cell electrodes (separated 2 mm) was 4.5 kV. The SH light was measured with two different photomultipliers, Hamamatsu R2949 for visible (532 nm) and R406 for near infrared (954 nm), respectively, and appropriate interference filters were used to remove the residual excitation light beyond the film and the NPP reference.

Polymer films were Corona poled to break the natural centrosymmetry of these systems. The films were held on a thermoregulated fixed stage for “*in situ*” SHG measurements at $1.91\text{ }\mu\text{m}$ during the poling process. The angle of incidence of the fundamental beam on the film was about 40° . A positive electric discharge was applied across the film using a standard Corona poling setup. A DC voltage of +5 kV was applied to a needle, perpendicular to the film. The distance between the needle and the film surface was about 1 cm. The poling process was performed as follows. The polymer films were heated at a rate of $5\text{ }^\circ\text{C/min}$ up to the optimal poling temperature with the electric field on and maintained in these conditions for 40 min. After several trials to avoid thermal decomposition and to control reproducibility of the process, $120\text{ }^\circ\text{C}$ for **Pol-PZ-CN** and $95\text{ }^\circ\text{C}$ for **Pol-O-CN** (g $56\text{ }^\circ\text{C}$ SmA $163\text{ }^\circ\text{C}$ I) were chosen as poling temperatures. Then, the films were cooled down to RT in the presence of the poling field, and finally, it was turned off. A quite sharp decay followed by a slower decrease of the SH signal is observed after switching the field off. This behavior has been associated with the neutralization of charges trapped at the film surface during Corona poling and with different relaxation processes.¹⁵

Once the films were poled as just described, Maker fringes were measured to obtain second order nonlinear coefficients (d_{ij}). The poled films were held on a stage which rotates around a vertical axis, perpendicular to light's plane of incidence so as to detect the SH intensity generated by the film as a function of the incidence angle for the two mentioned

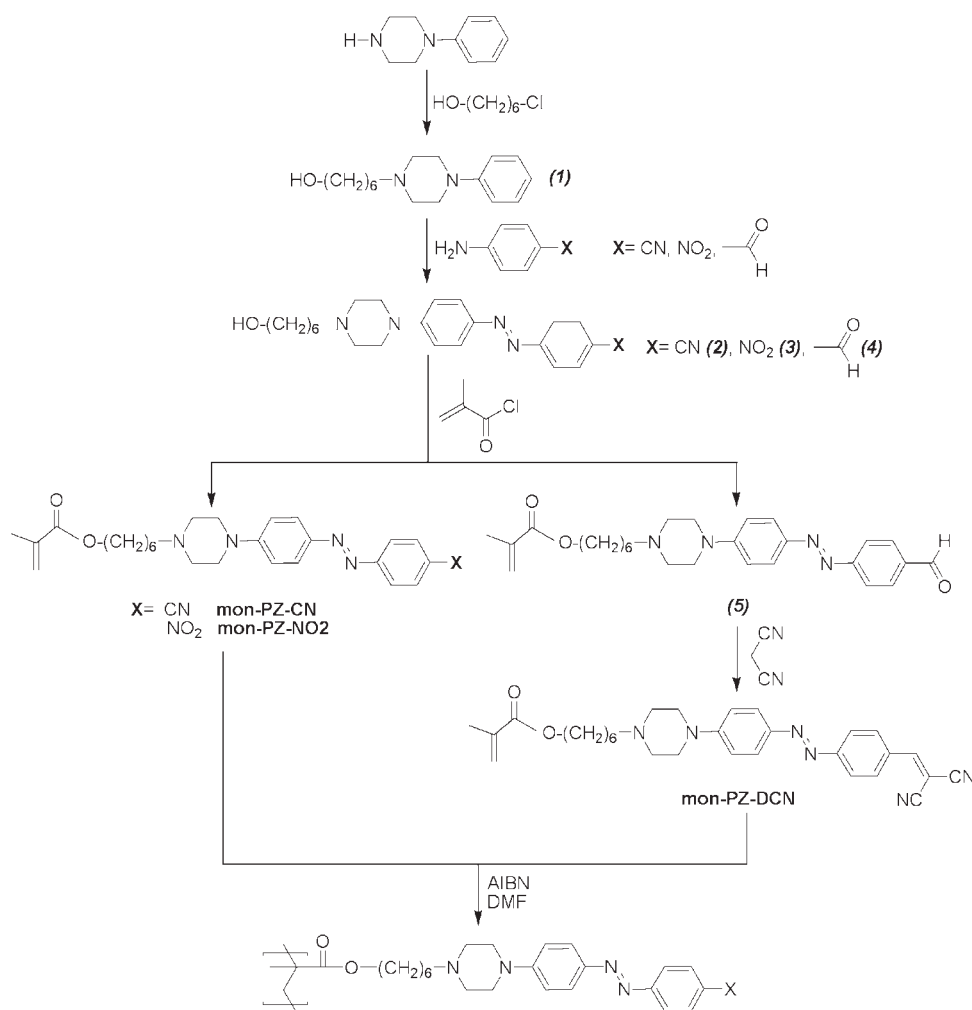


FIGURE 1 Synthetic pathway of monomers and polymers.

polarizations of the fundamental light. In general, poled films show $C_{\infty v}$ symmetry, and the nonlinear response is described by two independent d_{ij} coefficients, assuming Kleinmann symmetry conditions. So, two measurements using S and P polarized fundamental light are enough to obtain the experimental d_{31} and d_{33} values. In this work, the d_{31} coefficient has been deduced from the fitting of the harmonic signal obtained under excitation with S polarized light, and the d_{33} value has been calculated from measurements with P polarized light and using the d_{31} previously obtained. The analysis of the experimental curves (averaged from several runs at different points in the poled area) allowed us to obtain the nonlinear coefficients using a X-cut quartz crystal ($d_{11} = 0.35 \text{ pm/V}$ at $1.91 \mu\text{m}$) as a reference. The estimated error in d_{ij} values is $\pm 15\%$. Because of the noticeable difference between indices n_M and n_E measured in the films, the experimental Maker fringes were analyzed considering the work of Hayden and Herman,¹⁶ whose model takes into account film birefringence to calculate d_{ij} values. The refractive indices at 954 nm and $1.91 \mu\text{m}$ have been extrapolated from the guided mode measurements at 633 , 780 nm , and $1.31 \mu\text{m}$.

RESULTS AND DISCUSSION

Synthesis and Characterization

The monomeric dyes were prepared by azo coupling of N -(hydroxyhexyl)- N' -phenylpiperazine with the diazonium salts of 4-cyanoaniline, 4-nitroaniline and 4-aminobenzaldehyde and further esterification of the resulting azobenzene with methacryloyl chloride (Fig. 1). In the case of the dicyanovinyl derivative, the azomonomer (**5**), having a formyl group, was first synthesized and finally condensed with malonitrile (Knoevenagel reaction) to yield the monomer **mon-PZ-DCN**. Attempts to introduce the dicyanovinyl group in previous step lead to low yields.

It has been previously reported that N -methacryloyl- N' -phenylpiperazine and N' -phenylazophenyl derivatives are not prone to polymerize by a free radical polymerization.¹⁷ The steric hindrance of the N,N -dialkylmethacrylamide group was claimed as the reason for this failure of the polymerization. In our approach, the reactive group was separated from the piperazine ring by a flexible hexamethylenic spacer, which it has been widely used in the synthesis of reactive monomers for preparing side chain liquid crystalline polymers.

TABLE 1 Thermal and Mesomorphic Properties of Monomers

Compound	Phase Transitions (°C) ^a
mon-PZ-CN	K 120 (23.7) SmA 164 (0.4) N 179 (0.2) I polymerization
mon-PZ-NO₂	K 128 (22.7) SmA 179 (3.6) I polymerization
mon-PZ-DCN	K 136 (16.7) polymerization

^a Phase transitions were read at the onset temperature of peaks corresponding to first heating run at 10 °C/min. ΔH are indicated in brackets (kJ/mol).

Nevertheless, a relatively high amount of thermal initiator is required to polymerize these monomers with yields around 40%. However, similar monomers but without piperazine groups (ether linkage instead of the piperazine) were successfully polymerized in good yields and with high molecular weights under similar conditions.^{5(a,b)} The expected chemical structure of the synthesized polymers was confirmed by elemental analysis, infrared spectroscopy, and NMR. Polymer having a dicyanovinyl group **pol-PZ-DCN** was insoluble in common organic solvents once purified. Nevertheless, IR spectrum of this compound exhibits a band at 1672 cm⁻¹ corresponding to the terminal double bond, which remains when the polymer was heated up to temperatures around 225 °C. This result ruled out crosslinking of the terminal group as the cause of the insolubility of this material.

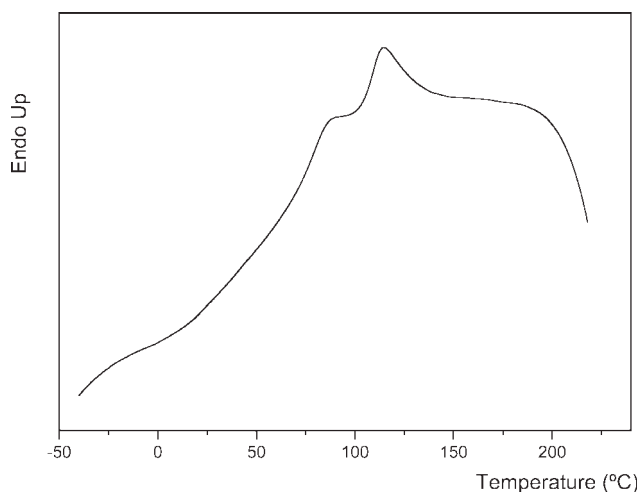
The thermal and mesomorphic properties of monomers are collected in Table 1. As it can be seen, all the monomers exhibit mesomorphism except in the case of **mon-PZ-DCN**, which polymerizes just above the melting transition and prevents mesomorphism to be adequately characterized. **Mon-PZ-CN** and **mon-PZ-NO₂** also polymerize around the isotropization transition temperature and exhibit a SmA phase. **Mon-PZ-CN** exhibits a short range of nematic phase as well. Thermal properties of polymers are gathered in Table 2. Polymers exhibit a lower thermal stability than analogous polymers having an oxygen atom instead of the piperazine group, and all polymers present weight loss at temperatures above 200 °C. This fact limits the observation of mesomor-

TABLE 2 Thermal Stability and Transition Temperatures of Polymers

Polymer	TGA Decomposition Temp. (°C) ^a	Phase Transitions (°C) ^b
pol-PZ-CN	245	g 77 K 114 SmA decomp $t > 200$
pol-PZ-NO₂	235	g 60 K 118 SmA decomp $t > 175$
pol-PZ-DCN	240	g 83 K 150 decomp $t > 170$

^a Onset of the decomposition process as detected on the thermogravimetric curve.

^b Data corresponding to the first heating scan.

**FIGURE 2** DSC trace corresponding to the first heating scan (10 °C/min) of **pol-PZ-CN**.

phic phases. Thus, **pol-PZ-CN** and **pol-PZ-NO₂** exhibit a mesomorphic phase having textures, which are indicative of a SmA phase. Both polymers are semicrystalline as prepared, but in the second heating scan only a glass transition is observed (when they are previously heated up to temperatures below thermal decomposition). Nevertheless, both polymers show evidences of decomposition above ~200 °C, as it can be detected by DSC and optical microscopy. In fact, an exotherm is observed around this temperature (see Fig. 2 as an example), and a darkening of the polymeric sample is observed under the microscope. However, **pol-PZ-DCN** did not exhibit softening or evidences of a fluid phase, and it decomposes above ~160 °C according to DSC traces (a broad exotherm is observed) and the optical microscopy observations.

Optical Characterization

UV-vis spectra of piperazine containing monomers have been measured in CH₂Cl₂ solutions, showing an intense band in the blue region, assigned to π - π^* transitions of trans azo isomers. The wavelengths of maximum absorption, λ_{max} , are 430, 460, and 490 nm for CN, NO₂, and DCN acceptors, respectively. λ_{max} for **mon-O-CN** in the same solvent is 365 nm. As expected, the substitution with stronger donor and acceptor terminal groups results in red shifted absorption bands.

Previously to the study of NLO response, the optical properties of **pol-PZ-CN** have been characterized and UV-vis spectra of thin fresh films have been measured at different incidence angles. As it can be seen in Figure 3, the spectrum at normal incidence shows a broad band with a marked peak at about 380 nm. If this spectrum is compared with that of a polymer solution, shown in the figure as well, a clear band broadening and blue shift of the absorption maximum are observed in the film. Hypsochromic shifts in azopolymer spectra are usually attributed to the aggregation of azobenzene chromophores. Similar absorption spectra, with a peak in the higher energy side of the band, have been reported by

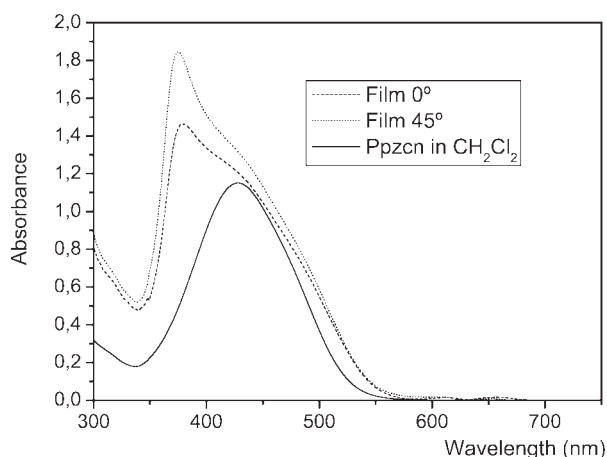


FIGURE 3 UV-vis spectra of **pol-PZ-CN** corresponding to CH_2Cl_2 solution and as prepared film. Measurements taken at normal and 45° incidence are shown.

several authors and associated with antiparallel H azo aggregates.^{18,19} On the other hand, higher absorption is observed when UV-vis spectra are taken at 45° when compared with those measured at normal incidence, once they are corrected by the longer path length at oblique incidence. So, the absorbance increase at 45° indicates an anisotropic molecular arrangement in the fresh films, where azo chromophores are rather oriented out-of-plane (homeotropically). This fact was confirmed by refractive index measurements, which revealed a difference $\Delta n = n_M - n_E$ of about 0.1 at 633 nm, as collected in Table 3. Indices corresponding to **pol-O-CN** films, in which a slighter homeotropic tendency was observed, are also included in Table 3. The initial homeotropic orientation experienced a noticeable increase on heating to temperatures within the mesophase range. Although the increase rate depends on the temperature, similar final values (up to 0.35) were achieved on heating **pol-PZ-CN** films. This fact can be associated with the thermotropic cooperative motion of azo groups, extensively described in the literature.²⁰ Most of the related published works concern the thermal amplification of the photoinduced in-plane anisotropy that occurs when photo-oriented azo LC polymer films are annealed at temperatures in the mesophase. However, it has been also described

TABLE 3 Refractive Indices Values (Averaged from Several Films) of the Polymers, Obtained by Waveguide Method at 633 nm After Different Treatments

Sample	Treatment	n_E	n_M
pol-PZ-CN ^{a,b}	Untreated	1.63	1.72
pol-PZ-CN ^a	Annealed at 120 °C	1.56	1.89
pol-PZ-CN ^a	Preirrad. 440 nm depol	1.65	1.76
pol-PZ-CN ^b	Preirrad. 440 nm depol	1.67	1.75
pol-O-CN	Fresh	1.63	1.64
pol-O-CN	Annealed at 90 °C	1.55	1.82

^a Film thickness: 1.2 μm .

^b Film thickness: 0.6 μm .

in several side chain azopolymers that side mesogens tended to form homeotropic domains when the sample was thermally annealed without being previously photooriented.²¹ To obtain a deeper insight about molecular arrangement in the thermally annealed films, UV-vis measurements were carried out after different time intervals at 120 °C. The absorbance spectra of a fresh film and the corresponding to the annealed one for 1 min at 120 °C are shown in Figure 4(a). The absorbance of the latter is clearly less intense, as expected if azo chromophores are oriented out-of-plane, but differences in the band shape are also observed. In particular, the band associated with azo aggregates has a higher relative weight with respect to the isolated chromophore's one. This spectral feature is stressed for rough thermal conditions. Aggregation favored by thermally enhanced homeotropic alignment has been reported.^{18,21(c,d),22}

The influence of UV-blue preirradiation on the optical properties of **pol-PZ-CN** has been explored. The effect of light in azo aggregate's breakage has been widely studied.^{18,23} The E-Z photoisomerization cycles of azo chromophores destroy

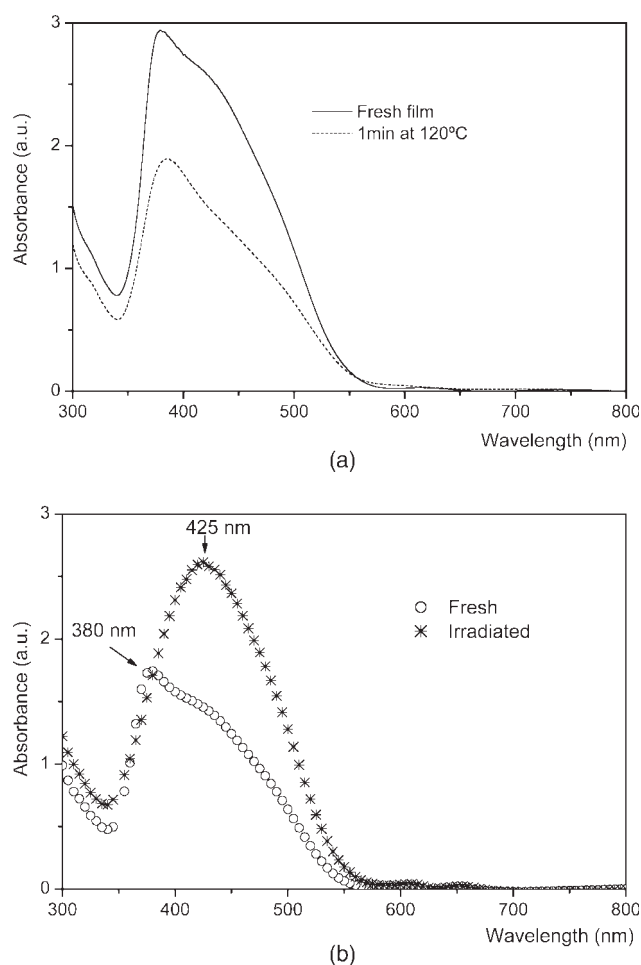


FIGURE 4 (a) UV-vis spectra of a film of **pol-PZ-CN** before and after annealing at 120 °C for 1 min, measured at normal incidence. (b) UV-vis spectra of a **pol-PZ-CN** film before and after irradiation with light, measured at normal incidence.

TABLE 4 Wavelength of Maximum Absorption, λ_{\max} and Values of $\mu\beta$ in CH_2Cl_2 , Determined from EFISH Measurements at 1.91 μm , and 1.06 μm When Possible. $\mu\beta(0)$ Values have been Deduced Using a Two Level Dispersion Model

Compound	λ_{\max} (nm)	$\mu\beta$ (10^{-48} esu) ^{a,b}	$\mu\beta(0)$ (10^{-48} esu)	$\mu\beta$ (10^{-48} esu) ^{a,c}	$\mu\beta(0)$ (10^{-48} esu)
mon-PZ-CN	430	950	280	340	260
mon-PZ-NO₂	460	— ^d	— ^d	440	320
mon-PZ-DCN	490	— ^d	— ^d	750	510
mon-O-CN	365	180	80	90	70

^a Experimental uncertainty in $\mu\beta$ values is estimated to be $\pm 15\%$.

^b Measurements performed at 1.06 μm .

^c Measurements performed at 1.91 μm .

^d The red shifted absorption spectra precluded the use of the 1.06 nm excitation.

the aggregate phase and the azo groups become isolated. Bearing in mind that the presence of nonpolar aggregates is detrimental for polar ordering, we planned to modify the aggregation state to study its influence on the poling process. So, **pol-PZ-CN** films were irradiated with light from a Hg lamp using a band-pass filter centered at 440 nm (45 mW/cm², BW: 100 nm). UV-vis absorption spectrum [Fig. 4(b)] at normal incidence shows the increase and red shifting of the absorption band, and aggregate's peak at 380 nm is not observed. The change in the shape evidences that a noticeable percentage of aggregates absorbing at 380 nm are broken on irradiation.

NLO Properties

The $\mu\beta$ values of monomeric precursors were obtained from EFISH measurements in CH_2Cl_2 at 1.91 μm . Molecular hyperpolarizabilities of **mon-PZ-CN** and **mon-O-CN** (both showing blue shifted absorption bands when compared with **mon-PZ-NO₂** and **-DCN** monomers) have also been measured at 1.06 μm . Slight absorption effects were observed in **mon-PZ-CN** EFISH fringes, so absorption coefficient $\alpha_{2\omega}$ was measured in solution and taking into account in data processing.²⁴ Experimental $\mu\beta$ and $\mu\beta(0)$ values deduced by using a simple two level dispersion model²⁵ are shown in Table 4. Very close $\mu\beta(0)$ values have been obtained from measurements performed at different wavelengths as predicted by two level model for rod shape dipolar chromophores. As expected, piperazine group gives rise to an enhancement of the molecular NLO response, which also increases with the strength of the acceptor moiety (**DCN** > **NO₂** > **CN**). The well-known standard Disperse Red 1 was measured in the same conditions obtaining $\mu\beta = 680 \times 10^{-48}$ and $\mu\beta(0) = 470 \times 10^{-48}$ esu. These results agree with those previously reported for a series of push-pull azobenzene dyes bearing a dialkylamino donor group and the mentioned electron withdrawing moieties among others.²⁶

The second order NLO properties of **pol-PZ-CN** films have been evaluated by second harmonic (SH) generation measurements. This polymer does not show an isotropic state under 200 °C, decomposition temperature (Table 2), so it was not possible to study thermally isotropized **pol-PZ-CN** films. Freshly made films, of about 1.2 μm thick, were poled

by applying the thermal poling process described in the “Experimental” section (up to 120 °C). Quite high SH intensity was detected during the “*in situ*” Corona poling process and a remarkable signal remained after switching the field off. To evaluate the temporal stability of the induced polar order, we measured the harmonic signal at different time intervals after finishing the poling process. In Figure 5, we show the evolution of the squared effective nonlinear coefficient, d_{eff} , normalized to the value measured about 2 h after switching the field off, for a variety of measured films. It can be seen in the figure that after a few days, a quite stable value of harmonic signal is measured, which stays essentially constant several weeks after the poling. This indicates that a noticeable degree of polar order remains in the films kept at RT. Concerning the thermal stability of the electric field induced polar ordering, we show in Figure 6 a typical evolution with temperature of SH signal. These measurements were carried out at least 2 weeks after finishing the poling process. Thermal stability was checked by heating samples near the mesophase range from RT at a rate of 5 °C/min. A decrease of the SH signal well above T_g was observed. The

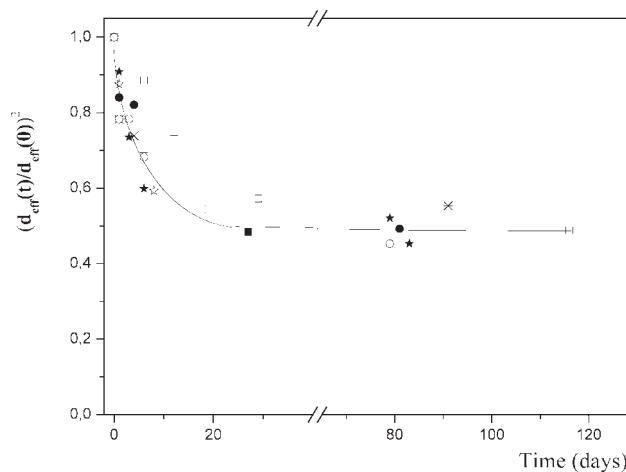


FIGURE 5 Temporal stability of SHG signal for several poled **pol-PZ-CN** films. The squared effective NLO coefficients are normalized to the value measured about 2 h after switching the field off.

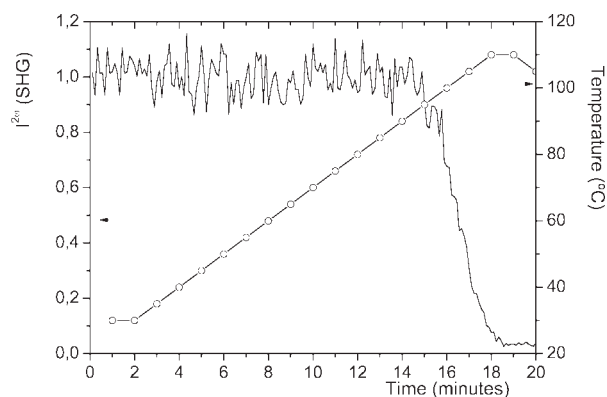


FIGURE 6 Second harmonic signal versus temperature for poled **pol-PZ-CN** film.

films were maintained at 110 °C for a short time, just until the disappearance of the harmonic signal. Under these conditions, new poling processes gave rise to NLO responses similar to those obtained for the first time.

The stable nonlinear coefficients of **pol-PZ-CN**, gathered in Table 5, were obtained from the fitting of the Maker fringes measured beyond 2 weeks after finishing the poling process. As correspond to $C_{\infty v}$ symmetry, the obtained Maker fringes were identical when the sample was rotated around an axis perpendicular to the film. In the case of films of about 1.2 μm thick, the nonlinear coefficients were $d_{31} = 1$ pm/V and $d_{33} = 8$ pm/V. These values are consistently higher than those obtained for a series of azo polymers with a weaker NLO chromophore (as **mon-O-CN** but with a spacer of two carbon atoms instead of six) previously studied in our group.^{5(b)} A value of $d_{33} = 26$ pm/V, larger than the obtained for **Pol-PZ-CN**, was reported for a side chain polymethacrylate functionalized with a similar azo chromophore, 4-dialkylamino-4'-cyanoazobenzene.²⁷ Nevertheless, the measurements were performed using 1.06 μm fundamental wavelength, so the reported d_{33} value is likely resonantly enhanced due to the proximity of the harmonic wavelength (532 nm) to the absorption of the side chain chromophore. On the other hand, clearly lower d_{33} values were reported¹² for polymethacrylates functionalized (ca., 30%) with similar or stronger NLO moieties, linked to the main chain, without

any spacer. The authors attributed the hardly effective poling to the hindered mobility of the nonlinear chromophores due to the rigidity of the side-chain structures.

As we have mentioned previously, the initial homeotropic orientation in **pol-PZ-CN** fresh films can be thermally enhanced by annealing in the mesophase. Some authors have stated that axial orientation of the NLO moieties can improve electric field-induced polar ordering,^{10,28} when compared with initially isotropic samples. However, we have clearly observed that in our system the homeotropic ordering is accompanied by an increase of aggregation. Therefore, the effect of the enhanced out-of-plane ordering of thermally annealed polymer samples on the NLO response was studied. The samples were annealed at 120 °C for 30 min (out-of-plane birefringence Δn (0.30)). Afterward, a poling process in the same conditions as the freshly made films was carried out, obtaining SHG signals clearly lower than those observed in the former. These results are consistent with the detrimental effect of the aggregation, which partially inhibits the noncentrosymmetric alignment under our experimental conditions.

The influence of the different strength of chromophore's dipole moment in NLO properties was more extensively studied, by comparing the results obtained for **pol-PZ-CN** with **pol-O-CN** films oriented in the same conditions. The lower d_{ij} values obtained (Table 5) for **pol-O-CN** are a result of the lower $\mu\beta$ value of the corresponding chromophore. The effect of the enhanced out-of-plane ordering of thermally annealed films in NLO properties was also studied on **pol-O-CN** resulting quite different to the behavior in **pol-PZ-CN** films. Although a noticeable axial order is also achieved by annealing the films at 95 °C ($\Delta n \geq 0.20$), the obtained SHG signals are similar for both of the initial states (untreated and annealed). These results could be associated with the lower **mon-O-CN** dipole moment values and consequently weaker aggregation tendency in **pol-O-CN** when compared with **pol-PZ-CN**. In both cases, homeotropic arrangement leading to an antiparallel alignment does not improve subsequent electric field induced polar alignment.

A comment should be done at this point about macroscopic response comparison between recently poled **pol-PZ-CN** ($d_{33} = 11$ pm/V) and **pol-O-CN** ($d_{33} = 6.5$ pm/V). The ratio between their respective coefficients is below the predicted

TABLE 5 Nonlinear Coefficients Measured for Polymer Films Poled After Different Treatments. The Coefficients have been Determined Beyond 2 Weeks After Finishing the Poling Process. The Refractive Index Values at 953 (n_E^{ω}) and 1907 nm (n_M^{ω}) Used in the Fitting Procedure were Extrapolated from Mode Coupling Measurements Performed at 633 and 1308 nm

Polymer Films	Treatment	Refractive Indexes				d_{ij} (pm/V)	
		n_E^{ω}	n_M^{ω}	$n_E^{2\omega}$	$n_M^{2\omega}$	d_{31}	d_{33}
pol-PZ-CN (1.2 μm)	Untreated	1.55	1.70	1.56	1.73	1	8.0
pol-PZ-CN (1.2 μm)	Preirrad. 440 nm depol	1.53	1.73	1.55	1.76	1	12
pol-PZ-CN (0.6 μm)	Untreated	1.55	1.72	1.56	1.74	1.3	10
pol-PZ-CN (0.6 μm)	Preirrad. 440 nm depol	1.53	1.78	1.54	1.80	1.1	14
pol-O-CN (1.2 μm)	Untreated	1.56	1.70	1.57	1.73	0.5	3.5

one using the expression $d_{33} = N \beta_{zzz}^* \langle \cos^3 \theta \rangle$.⁷ N is the number density, β_{zzz}^* is the microscopic hyperpolarizability incorporating local field factors, and $\langle \cos^3 \theta \rangle$ is the axial order parameter, being θ the angle between chromophore axis and poling direction. Different models have been used to analytically evaluate the order parameter, from the simplest isotropic poled polymer⁷ one to effective field approaches,⁶ which include the effect of a chromophore on another. In the last, dipole moment and distance between chromophores are two key parameters, leading to a reduction of the maximum achievable polar order. In our case, the intensity of dipole-dipole interactions in **pol-O-CN** and **pol-PZ-CN** is probably different and side chain chromophores tend to adopt antiparallel conformations, with closeness depending on their dipole moment. These internal forces work in opposition to the electric field external one, hindering at different extents polar orientation, and contributing to the observed difference between the two polymers. The assumption of stronger interactions in **pol-PZ-CN** is supported by the relevant presence of H aggregates, even in fresh films, (Fig. 3) which becomes more important after thermal treatments. It has been reported that these nonpolar aggregates, caused by the strong dipole-dipole interaction, cannot be oriented by the applied electric field.⁶

Considering the later, we planned to reduce aggregation in **pol-PZ-CN**, to achieve a higher polar order. Firstly, the disruption of aggregates was carried out by the irradiation of 1.2 μm thick films with UV-blue light (Hg lamp). Samples were subsequently poled following the same described process for fresh and annealed films. A faster increase and an enhanced NLO response were observed “*in situ*” during the poling process, supporting our assumption about the hindered polar ordering of aggregates. As it can be seen in Table 5, the d_{ij} values measured confirm the difference. As the response after irradiation was higher, we tried to optimize our results using thinner films. Freshly made and irradiated samples of about 0.6 μm thick were poled. High enough NLO efficiency was achieved by reducing thickness and by irradiating. The obtained d_{ij} coefficients for recently poled preirradiated thin films were $d_{33} = 17$ and $d_{31} = 1.3$ pm/V, and in the case of as prepared ones, the results were $d_{33} = 13$ pm/V and $d_{31} = 1.7$ pm/V. In Table 5, we report the stable d_{ij} values and the refractive indices extrapolated from measurements in the irradiated and poled zone. These results show that larger d_{33} values and d_{33}/d_{31} ratios are obtained on irradiation. This ratio is predicted to be 3 by the thermodynamic model for isotropic materials poled under low electric field conditions.⁷ Ratio values higher than 3, as ours, have been mainly associated with higher polar order due to intense poling electric fields²⁹ or to chromophore interactions dealing to favor high axial ordered states, as several authors reported in side chain liquid crystalline polymers.^{10,28} As for the field strength, low content DR1 doped PMMA were poled in the same conditions, giving rise to $d_{33}/d_{31} \approx 3$. On the other hand, the existence of a noticeable axial order has been demonstrated by the aforementioned out-of-plane birefringence values. Δn values as high as 0.2 for untreated films and

0.3 for the irradiated ones have been measured at 633 nm, in the poled zone. However, we have found that this birefringence in **pol-PZ-CN** is caused by both the polar order and the homeotropic ordering tendency shown by nonpolar aggregates. In fact, clearly bigger Δn values have been measured out of the poled zone, which has been subjected to the same thermal conditions. On the other hand, SHG signal time decay does not go along with a significant Δn decrease and, in addition, just after thermal removal of the SHG signal (Fig. 6) a consistent decrease of Δn has not been detected.

The lower Δn values measured in the poled zone, and the optical spectra, suggest that the electric field inhibits (at least partially) the antiparallel axial ordering tendency of azo chromophores³⁰ leading to a certain degree of polar order.

Finally, it is worth to say that, although poling of **pol-PZ-CN** presents some of the handicaps reported for smectic A polymer, quite high and stable nonlinear response was achieved. These results would be most likely overcome by using copolymers with reduced piperazine moiety content.

CONCLUSIONS

The molecular nonlinearities of a series of chromophores bearing piperazine as donor group and several acceptor groups have been measured. $\mu\beta$ values have shown the expected tendency considering the strength of the withdrawing groups (**DCN** > **NO₂** > **CN**).

Smectic liquid crystal polymer having a terminal cyano group in the side chain chromophore (**pol-PZ-CN**) formed thin films with good optical quality. However, formation of aggregates proceeds from film production by casting, as it can be detected in the absorption spectra. These azobenzene aggregates are enhanced by heating up to temperatures within the mesophase range of the polymer. On the other hand, irradiation with UV-vis light has been associated with their breakage. Corona poling process induces stable polar order of chromophores and consequently thin films show a settled NLO response. The axial order achieved is due to both polar and nonpolar arrangement of the NLO moieties, as a result of the competition between external electric field effect and interchromophore interactions. The obtained d_{ij} values are lower than the potentially achievable ones, taking into account the $\mu\beta$ values of the chromophores. Aggregation favored by dipole-dipole interactions represents a major factor in determining the macroscopic response of the system. This statement is supported by the noticeable increase of the NLO response observed when, to disrupt aggregates, thin **pol-PZ-CN** films are irradiated before the electric field poling process. Moreover, it has been reinforced by the lower SHG obtained when the out-of-plane arrangement is forced by the previous annealing at the mesophase.

The stability of the light improved nonlinear response has been checked several months after the poling, remaining at least the 50% of the initial harmonic signal.

Financial support from MICINN-FEDER (MAT2008-06522-C02-01 and -02) and Gobierno de Aragón-Fondo Social

Europeo (E39) is gratefully acknowledged. R. Alicante thanks the Spanish Government for a grant (FPI program, No. BES2006-12104).

REFERENCES AND NOTES

- (a) Burland, D. M.; Miller, R. D.; Walsh, C. A. *Chem Rev* 1994, 94, 31–75; (b) Nalwa, H. S.; Miyata, S. In *Nonlinear Optics of Organic Molecules and Polymers*; CRC Press: Boca Raton, 1997; Chapter 7, pp 128–309; (c) Samyn C.; Verbiest, T.; Persoons, A.; *Macromol Rapid Commun* 2000, 21, 1–15; (d) Cho, M. J.; Choi, D. H.; Sullivan, P. A.; Akelaitis, A. J. P.; Dalton, L. R. *Prog Polym Sci* 2008, 33, 1013–1058.
- (a) Delaire, J. A.; Nakatani, K. *Chem Rev* 2000, 100, 1817–1845; (b) Yesodha, S. K.; Sadashiva-Pillai, C. K.; Tsutsumi, N. *Prog Polym Sci* 2004, 29, 45–74.
- (a) Kumar, G. S.; Neckers, D. C. *Chem Rev* 1989, 89, 1915–1925; (b) Xie, S.; Natansohn, A.; Rochon, P. *Chem Mater* 1993, 5, 403–411; (c) Natansohn, A.; Rochon, P. *Adv Mater* 1999, 11, 1387–1391; (d) Sekkat, Z. In *Photoreactive Organic Thin Films*; Sekkat, Z.; Knoll, W., Eds.; Academic Press: San Diego, 2002; Chapter 8, pp 271–287; (e) Natansohn, A.; Rochon, P. *Chem Rev*, 2002, 102, 4139–4176.
- (a) Sekkat, Z.; Dumont, M. *Appl Phys B*, 1992, 54, 486–489; (b) Blanchard, P. M.; Mitchell, G. R. *Appl Phys Lett* 1993, 63, 2038–2040; (c) Sekkat, Z.; Kang, C. S.; Aust, E. F.; Wegner, G.; Knoll, W. *Chem Mater* 1995, 7, 142–147; (d) Sekkat, Z.; Prêtre, P.; Knoesen, A.; Volksen, W.; Lee, V. Y.; Miller, R. D.; Wood, J.; Knoll, W. *J Opt Soc Am B* 1998, 15, 401–413.
- (a) Sánchez, C.; Cases, R.; Alcalá, R.; López, A.; Quintanilla, M.; Oriol, L.; Millaruelo, M. J. *Appl Phys* 2001, 89, 5299–5306; (b) Rodríguez, F. J.; Sánchez, C.; Villacampa, B.; Alcalá, R.; Cases, R.; Millaruelo, M.; Oriol L. *Polymer* 2004, 45, 2341–2348.
- (a) Dalton, L. R.; Harper A. W.; Robinson B. H. *Proc Natl Acad Sci USA* 1997, 94, 4842–4847; (b) Dalton, L. R.; Steier, W. H.; Robinson, B. H.; Zang, C.; Ren, A.; Garner, S.; Chen, A.; Londergan, T.; Irwin, L.; Carlson, B.; Fifield, L.; Phelan, G.; Kincaid, C.; Amend, J.; Jen, A. J. *Mater Chem* 1999, 9, 1905–1920; (c) Wüthner, F.; Wortmann, R.; Meerholz, K. *Chem Phys Chem* 2002, 3, 17–31; (d) Pereverzev, Y. V.; Prezhdo, O. V.; Dalton, L. R. *Chem Phys Chem* 2004, 5, 1821–1830; (e) Yager, K. G.; Barrett, C. J. In *Polymeric Nanostructures and Their Applications*; Nalwa, H. S., Ed.; American Scientific Publishers: New York, 2006; Chapter 8, pp 1–38.
- Williams, D. J. In *Nonlinear Optical Properties of Organic Molecules and Crystals*; Chemla, D. A.; Zyss, J., Eds.; Academic Press: Orlando, FL, 1987; Vol. 1, Chapter II-7, pp 405–434.
- (a) Beltrani, T.; Bösch, M.; Centore, R.; Concilio, S.; Günter, P.; Sirigu, A. *J Polym Sci Pol Chem* 2001, 39, 1162–1168; (b) Carella, A.; Casalboni, M.; Centore, R.; Fusco, S.; Noce, C.; Quatela, A.; Peluso, A.; Sirigu, A. *Opt Mater* 2007, 30, 473–477; (c) Lanzi, M.; Paganin, L.; Cesari, G. *Macromol Chem Phys* 2008, 209, 375–384.
- (a) Meredith, G. R.; Vandusen, J. G.; Williams, D. J. In *Nonlinear Optical Properties of Organic and Polymeric Materials*; Williams, D. J., Ed.; Washington: ACS Symposium Series, 1983; Chapter 5, pp 109–133; (b) Singer, K. D.; Kuzlyk, N. G.; Sohn, J. E. *J Opt Soc Am B* 1987, 4, 968–976; (c) Van der Vorst, C. P. J. M.; Picken, S. J. *J Opt Soc Am B* 1990, 7, 320–325.
- (a) Amano, M.; Kaino, T.; Yamamoto, F.; Takeuchi, Y. *Mol Cryst Liq Cryst* 1990, 182A, 81–90; (b) Dubois, C.; Le Barry, P.; Mauzac, M.; Noël, C. *Acta Polym* 1997, 48, 47–87; (c) Kajzar, F.; Noël, C. *Adv Mater Opt Electron* 1998, 8, 247–262.
- Rau, I.; Kajzar, F. *Thin Solid Films* 2008, 516, 8880–8886.
- Tirelli, N.; Altomare, A.; Solaro, R.; Ciardelli, F.; Follonier, S.; Bosshard Ch.; Günter, P. *Polymer* 2000, 41, 415–421.
- Altomare, A.; Andruzzi, L.; Ciardelli, R.; Solaro, F.; Tirelli, N. *Macromol Chem Phys* 1999, 200, 601–608.
- Woo, H. Y.; Shim, H. K.; Lee, K. S. *Macromol Chem Phys* 1998, 199, 1427–1433.
- (a) Hampsch, H.; Torkelson, J.; Bethke, S.; Grubb, J. *J Appl Phys* 1990, 67, 1037–1040; (b) Wang, H.; Jarnegin, R. C.; Samulski, E. T. *Macromolecules* 1994, 27, 4705–4713; (c) Weyrauch, T.; Haase, W. In *Relaxation Phenomena. Liquid Crystals, Magnetic Systems, Polymers, High-Tc Superconductors, Metallic Glasses*; Haase, W.; Wróbel, S., Eds.; Springer: Berlin, 2003; Chapter 12, pp 667–691.
- Herman, W. N.; Hayden, L. M. *J Opt Soc Am B* 1995, 12, 416–427.
- Tirelli, N.; Suter, U. W.; Altomare, A.; Solaro, R.; Ciardelli, F.; Follonier, S.; Bosshard, Ch.; Günter, P. *Macromolecules* 1998, 31, 2152–2159.
- (a) Menzel, H.; Weichart, B.; Schmidt, A.; Paul, S.; Knoll, W.; Stumpe, J.; Fischer, T. *Langmuir* 1994, 10, 1926–1933; (b) Stumpe, J.; Fischer, Th.; Menzel, H. *Macromolecules* 1996, 29, 2831–2842; (c) Geue, Th.; Ziegler, A.; Stumpe, J. *Macromolecules* 1997, 30, 5729.
- (a) Lagugné-Labarthe, F.; Freibert, S.; Pellerin, C.; Pézolet, M.; Natansohn, A.; Rochon, P. *Macromolecules* 2000, 33, 6815–6823; (b) Freibert, S.; Lagugné-Labarthe, F.; Rochon, P.; Natansohn, A. *Can J Chem* 2004, 82, 1–10.
- (a) Fischer, Th.; Läsker, L.; Czaplá, S.; Rübner, J.; Stumpe, J. *Mol Cryst Liq Cryst* 1997, 298, 213–220; (b) Meier, J. G.; Ruhmann, R.; Stumpe, J. *Macromolecules* 2000, 33, 843–850; (c) Kidowaki, M.; Fujiwara, T.; Morino, S.; Ichimura, K.; Stumpe, J. *Appl Phys Lett* 2000, 76, 1377–1379.
- (a) Han M.; Morino S.; Ichimura K. *Macromolecules* 2000, 33, 6360–6371; (b) Cojocariu, C.; Rochon, P. *Pure Appl Chem* 2004, 76, 1479–1497; (c) Cojocariu, C.; Rochon, P. *Macromolecules* 2005, 38, 9526–9538; (d) Bobrovsky, A.; Shibaev, V.; Hamplova, V.; Kaspar, M.; Glogarova, M. *Monatsh Chem* 2009, 140, 789–799.
- Geue, T. M.; Pietsch, U.; Haferkorn, J. J.; Stumpe, J.; Date, R. W.; Fawcett, A. H. *Mol Cryst Liq Cryst* 1999, 329, 113–119.
- Rodríguez, F. J.; Sánchez, C.; Villacampa, B.; Alcalá, R.; Cases, R.; Col-lados, M. V.; Hvilsted, S.; Strange, M. *Polymer* 2004, 45, 6003–6012.
- Oudar J. L. *J Chem Phys* 1977, 67, 446–457.
- Oudar, J. L.; Chemla, D. S. *J Chem Phys* 1977, 66, 2664–2668.
- Tirelli, N.; Altomare, A.; Solaro, R.; Ciardelli, F.; Meier, U.; Bosshard Ch.; Günter, P. *J Prakt Chem* 1998, 340, 122–128.
- S'Heeren, G.; Persoons, A.; Rondou, P.; Wiersman, J.; Van Beylen, M.; Samyn, C. *Makromol Chem* 1993, 194, 1733–1744.
- Gonin, D.; Guichart, B.; Noël, C. *Macromol Symp* 1995, 96, 185–206.
- (a) Eich, M.; Sen, A.; Looser, H.; Bjorklund, G. C.; Swalen, J. D.; Twieg, R.; Yoon, D. Y. *J Appl Phys* 1989, 66, 2559–2567; (b) Rodríguez, V.; Lagugné-Labarthe, F.; Sourisseau C. *Appl Spectrosc* 2003, 59, 322–328.
- (a) Wortmann, R.; Rösch, U.; Redi-Abshiro, M.; Würthner, F. *Angew Chem Int Ed* 2003, 42, 2080–2083; (b) Vembris, A.; Rutkis, M.; Lai-zane, E. *Mol Cryst Liq Cryst* 2008, 485, 125–132.